

Electronic Supplementary Information

PdAg nanoparticles and aminopolymer confined within mesoporous hollow carbon spheres as an efficient catalyst for hydrogenation of CO₂ to formate

*Guoxiang Yang,^a Yasutaka Kuwahara,^{abc} Shinya Masuda,^a Kohsuke Mori,^{ab} Catherine Louis,^d and Hiromi Yamashita^{*ab}*

^a Division of Materials and Manufacturing Science, Graduate School of Engineering,
Osaka University, 2-1 Yamada-oka, Suita, Osaka 565-0871, Japan

^b Unit of Elements Strategy Initiative for Catalysts & Batteries (ESICB), Kyoto
University, Katsura, Kyoto 615-8520, Japan

^c JST, PRESTO, 4-1-8 Honcho, Kawaguchi, Saitama 332-0012, Japan

^d Sorbonne Universités, UPMC Univ Paris 06, UMR CNRS 7197, Laboratoire de
Réactivité de Surface, 4 Place Jussieu, Tour 43-33, 3ème étage, Case 178, F-75252
Paris, France

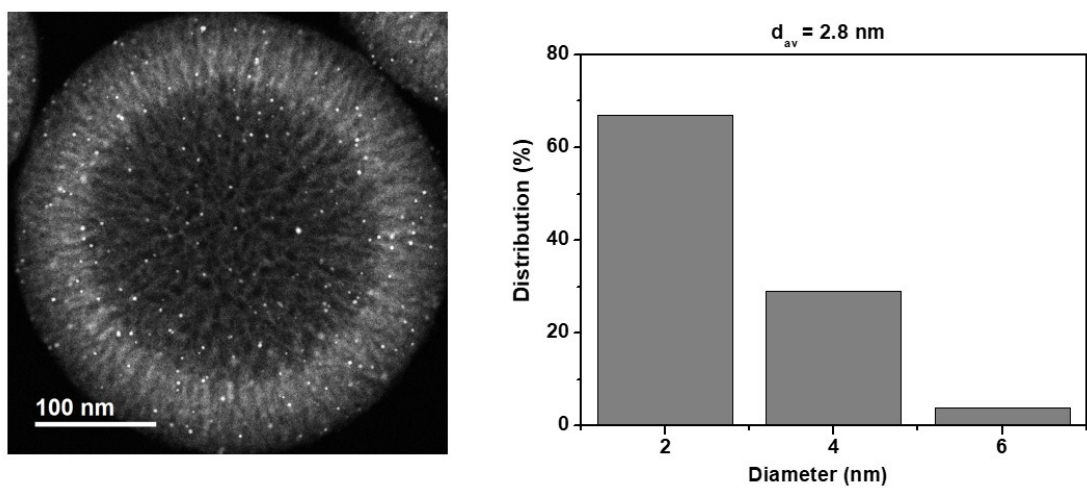


Figure S1. Particle size distribution for STEM images of $\text{Pd}_2\text{Ag}_8@\text{MHCS}$.

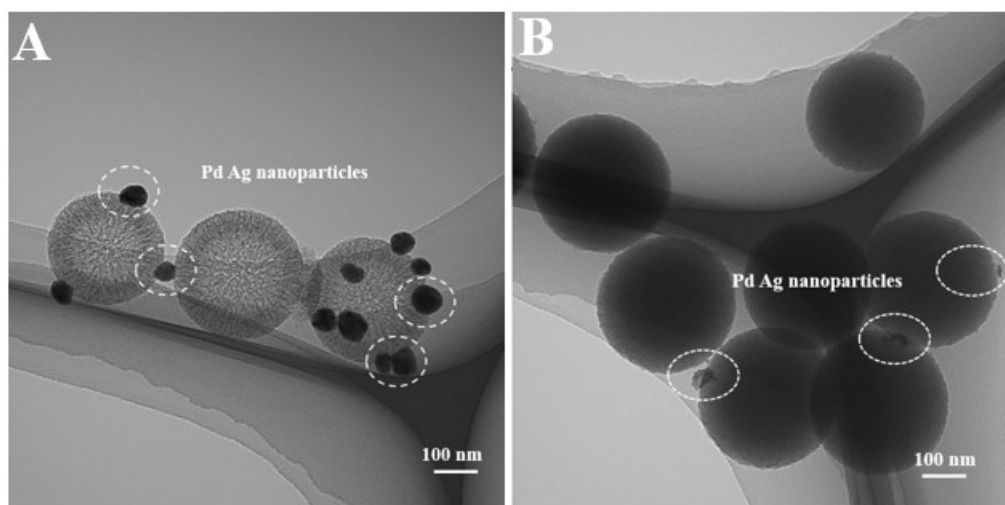


Figure S2. TEM images of (A) $\text{Pd}_2\text{Ag}_8@\text{MHCS}$, (B) $\text{Pd}_2\text{Ag}_8\text{-P}@\text{MHCS}$ without removal SiO_2 .

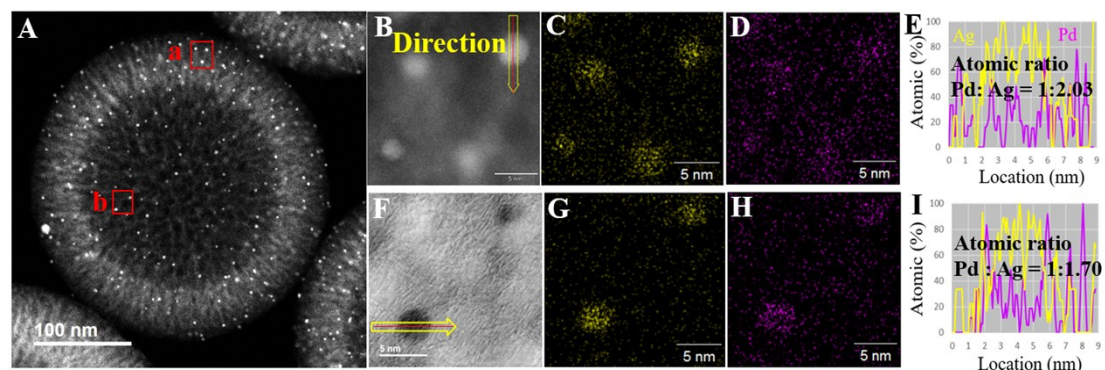


Figure S3. (A) STEM image of $\text{Pd}_2\text{Ag}_8\text{-P}@\text{MHCS}$, (B) STEM image of enlarged picture of the a zone red frame in Figure S2 (A), (C-D) the corresponding STEM elemental maps of (C) Ag, (D) Pd of PdAg alloy nanoparticles, (E) STEM elemental line scan across the PdAg alloy nanoparticles in (B), (F) STEM image of enlarged picture of the b zone red frame in Figure S2 (A), (G-H) the corresponding STEM elemental maps of (G) Ag (H) Pd of PdAg alloy nanoparticles, (E) STEM elemental line scan across the PdAg alloy nanoparticles in (F).

Table S1. The XRD size of $\text{Pd}_2\text{Ag}_8\text{-P@MHCS}$ and Ag-P@MHCS .

Sample	Ag content [wt%]	XRD size [nm]
$\text{Pd}_2\text{Ag}_8\text{-P@MHCS}$	4	37.8
Ag-P@MHCS	4	39.2

Table S2. Table 1. BET surface Area (S_{BET}), Total Pore Volume (Vp), Average Mesopore Diameter (Dave) of different catalysts.

catalysts	S_{BET} [m^2g^{-1}]	Vp [cm^3g^{-1}]	Dave [nm]
MHCS	1269	3.1	7.1
P@MHCS	814	1.4	5.5
Ag-P@MHCS	633	1.4	4.8
Pd-P@MHCS	619	1.4	4.8
Pd2Ag8-P@MHCS	666	1.5	4.8

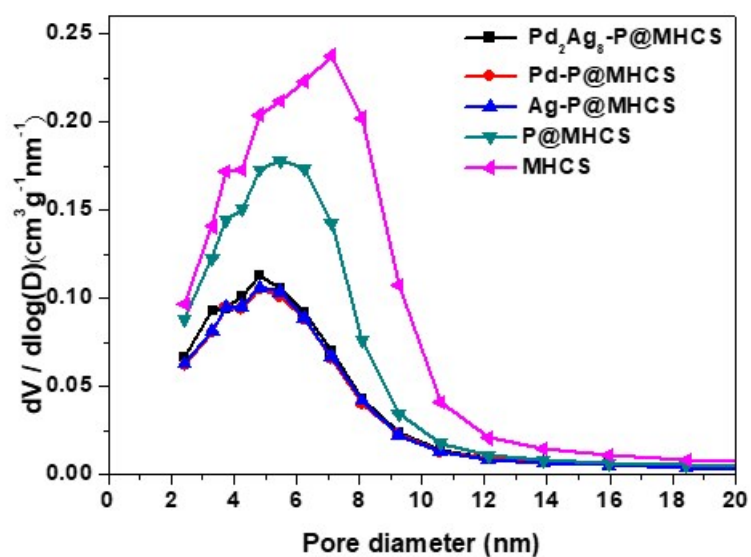


Figure S4. mesopore size distribution of $\text{Pd}_2\text{Ag}_8\text{-P@MHCS}$, Pd-P@MHCS , Ag-P@MHCS , P@MHCS and MHCS .

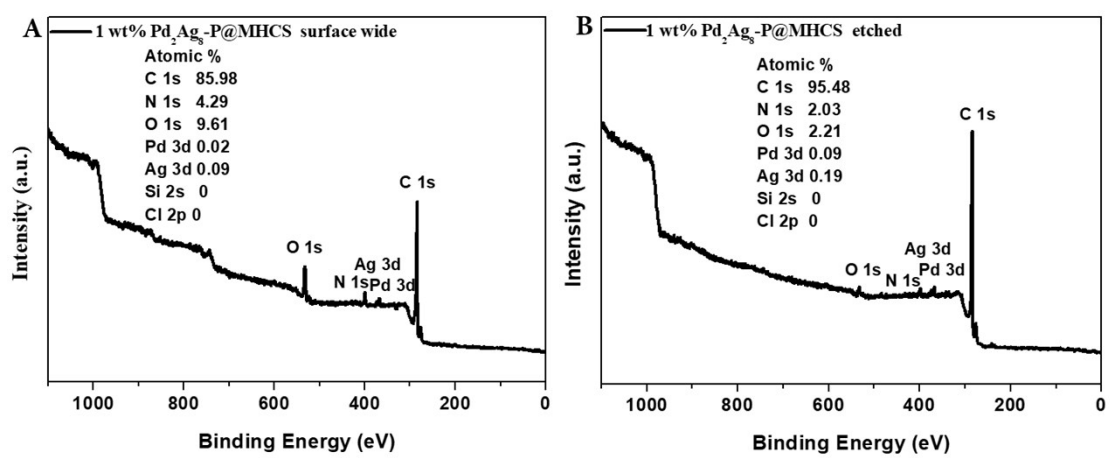


Figure S5. Survey spectrum of $\text{Pd}_2\text{Ag}_8\text{-P@MHCS}$ (A) surface wide and (B) etched.

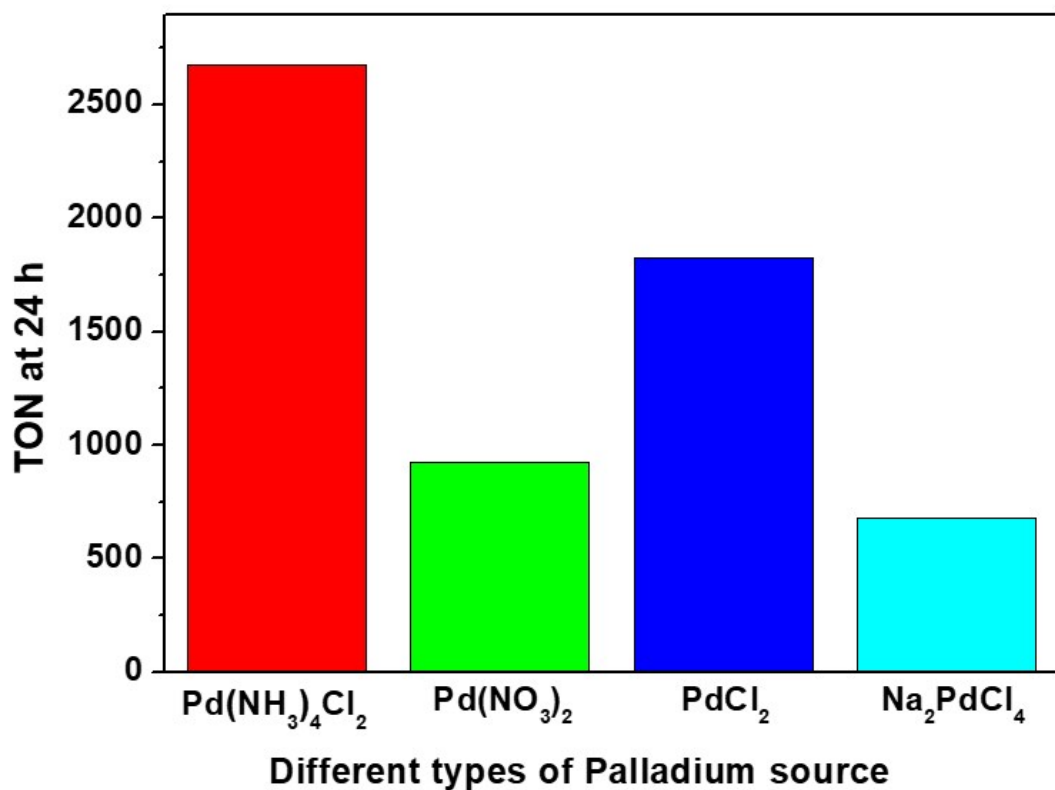


Figure S6. Effect of different types of Palladium source of $\text{Pd}_2\text{Ag}_8\text{-P@MHCS}$, Pd theoretical weight was 1 wt%, PdAg alloy mole ratio (Pd: Ag = 2:8) were prepared at different types of Pd source with AgNO_3 . Reaction conditions: catalyst (10 mg), 1.0 M aqueous NaHCO_3 solution (15 mL), H_2/CO_2 (1:1), total 2.0 MPa, 24 h.

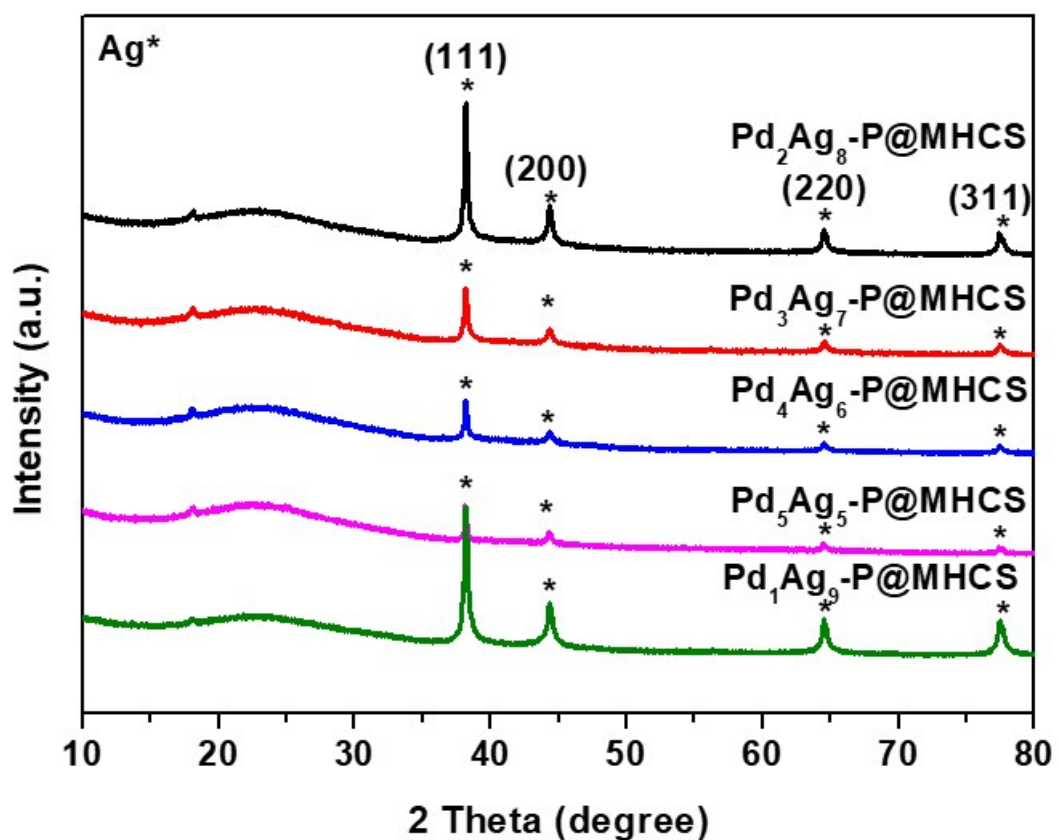


Figure S7. Powder XRD patterns of different molar ratio of PdAg-P@MHCS (Pd weight was 1 wt%).

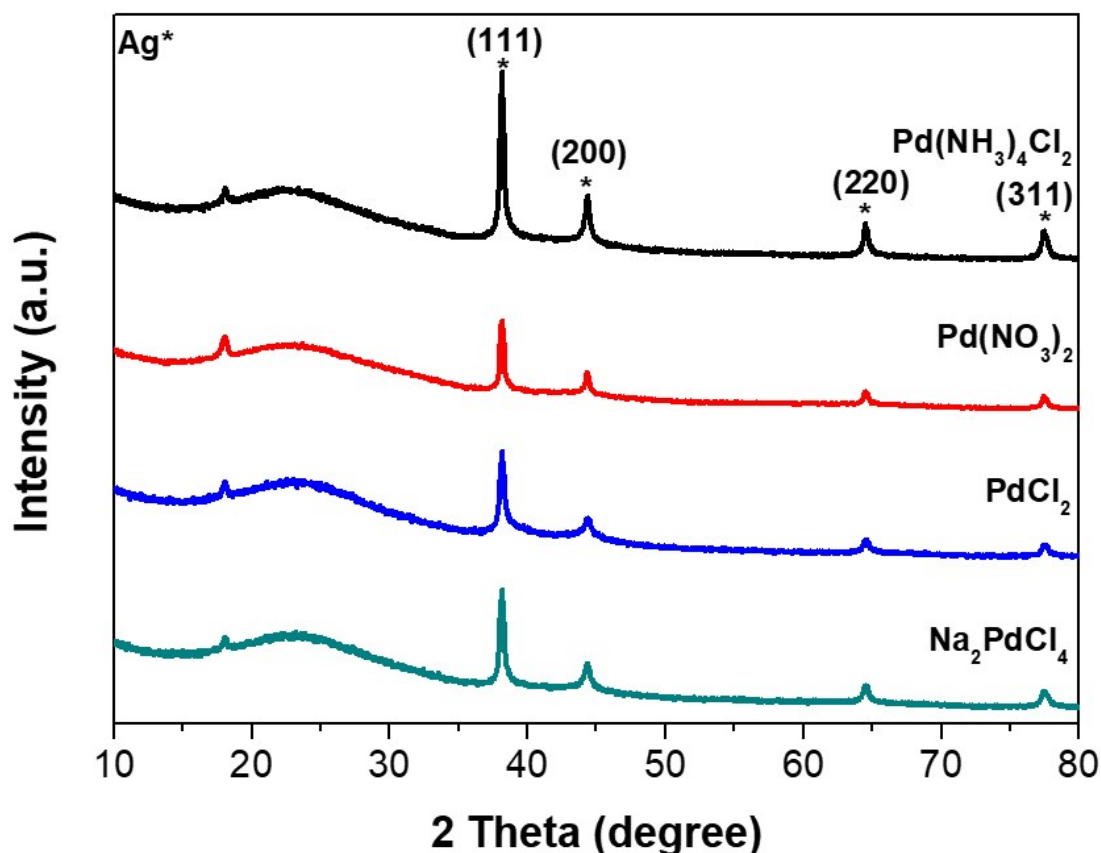


Figure S8. Powder XRD patterns of different types of Pd source of $\text{Pd}_2\text{Ag}_8\text{-P@MHCS}$ (Pd weight was 1 wt%). Pd theoretical weight was 1 wt%, PdAg alloy mole ratio (Pd: Ag = 2:8) were prepared at different types of Pd source with AgNO_3 .

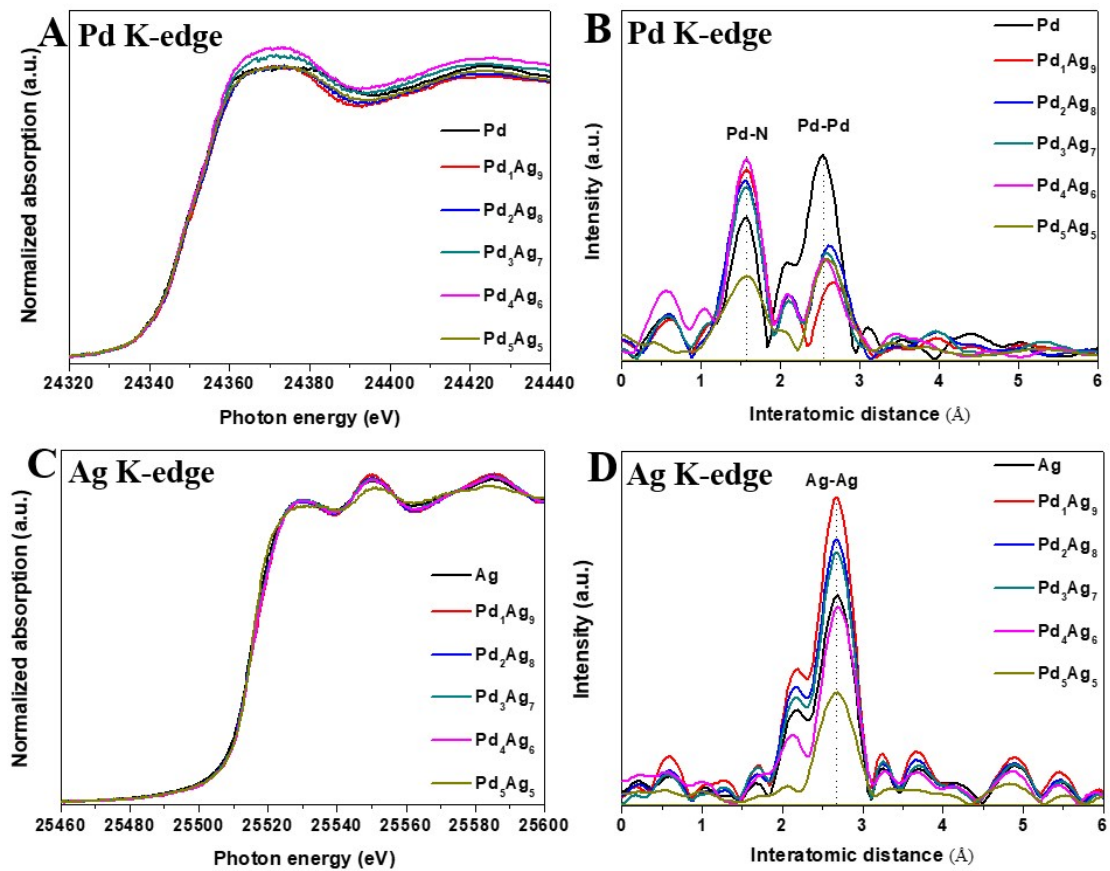


Figure S9. (A) XANES of Pd K-edge (B) Pd K-edge Fourier transforms EXAFS (C) XANES of Ag K-edge and (D) Ag K-edge EXAFS for different molar ratio of PdAg-P@MHCS.

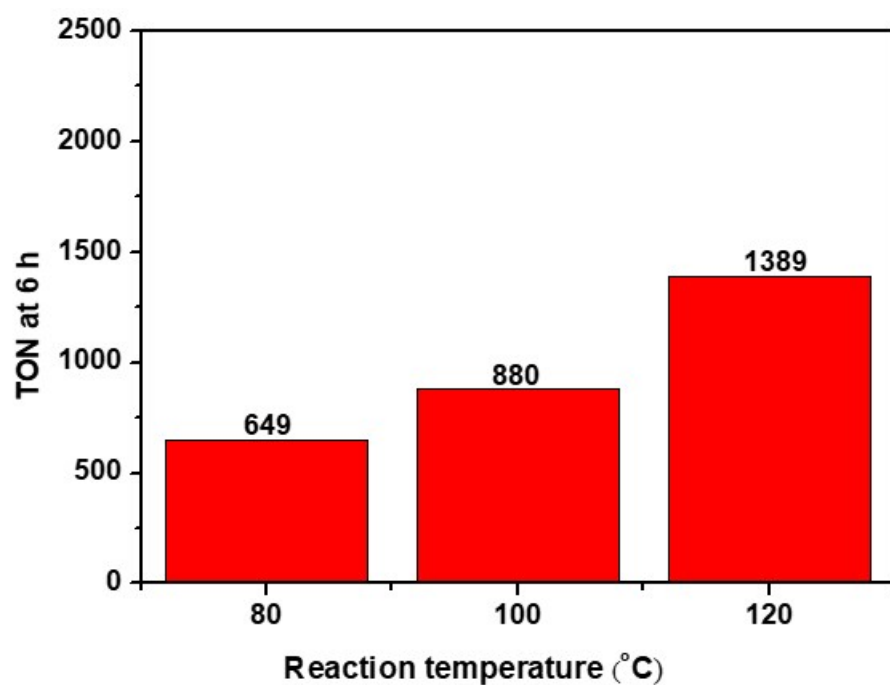


Figure S10. Effect of reaction temperature Reaction conditions: catalyst (10 mg), 1.0 M aqueous NaHCO₃ solution (15 mL), H₂/CO₂ (1:1), total 2.0 MPa, 6 h.

Table S3. The Pd contents of different molar ratio on PdAg alloy @ MHCS-TPOS catalysts as determined from ICP data.

Sample	Pd content [wt%]
Pd ₁ Ag ₉ -P@MHCS	1.15
Pd ₂ Ag ₈ -P@MHCS	0.95
Pd ₃ Ag ₇ -P@MHCS	1.08
Pd ₄ Ag ₆ -P@MHCS	1.02

Table S4. The N concentrations in the different content polymer of MHCS as determined by CHN elemental analysis.

Sample	N content [wt%]
MHCS	1.88
0.5P@MHCS	5.42
P@MHCS	8.58
2P@MHCS	9.68

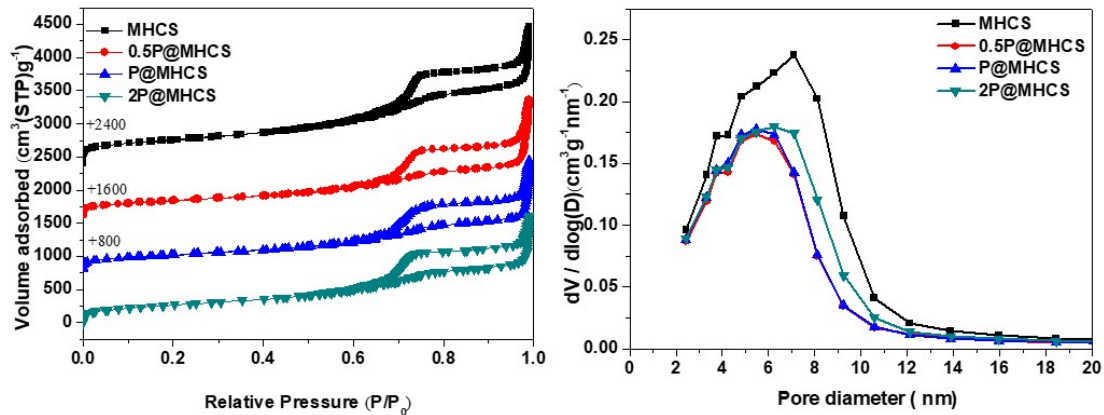


Figure S11. N_2 adsorption-desorption isotherms and mesopore size distribution of MHCS, 0.5P@MHCS, P@MHCS, 2P@MHCS.

Table S5. BET surface Area (S), Total Pore Volume (Vp), Average Mesopore Diameter (Dave) of different Catalysts.

catalysts	$S_{\text{BET}} [\text{m}^2\text{g}^{-1}]$	$V_p [\text{cm}^3\text{g}^{-1}]$	Dave [nm]
MHCS	1269	3.1	7.1
0.5P@MHCS	857	1.4	5.5
P@MHCS	814	1.4	5.5
2P@MHCS	764	1.3	5.7

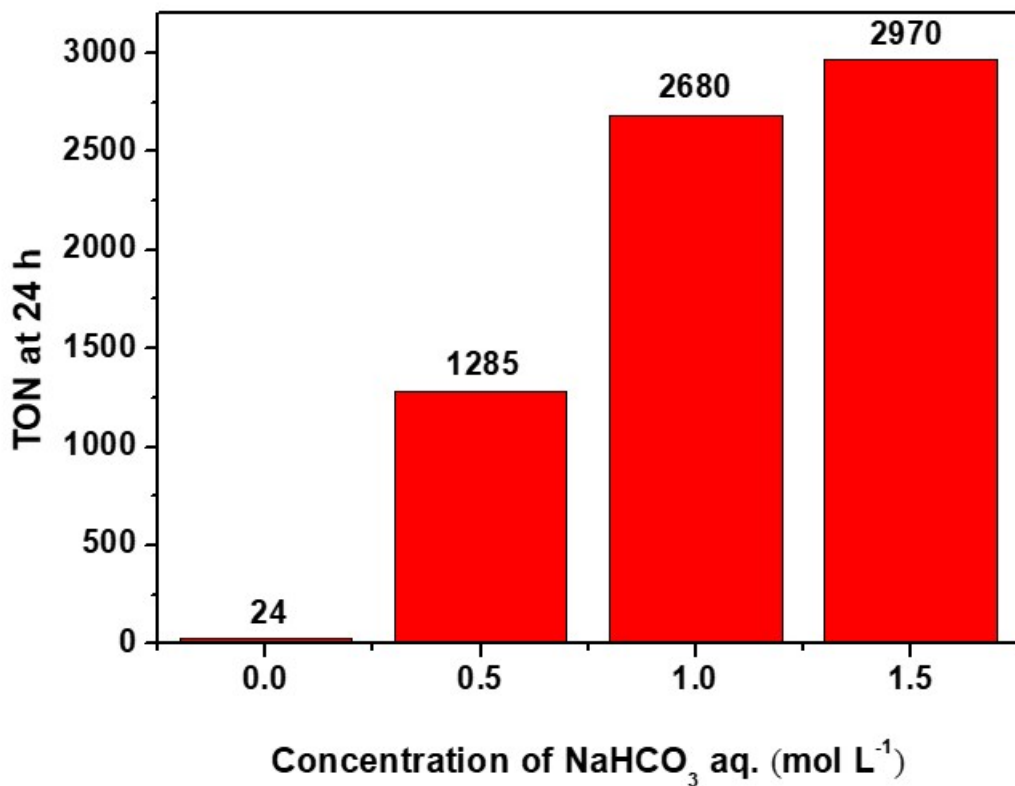


Figure S12. Effect of concentration of NaHCO_3 aqueous solution. Reaction conditions: 10 mg $\text{Pd}_2\text{Ag}_8\text{-P}@\text{MHCS}$, 1.0 M aqueous NaHCO_3 solution (15 mL), H_2/CO_2 (1:1, total 2.0 MPa), 100 °C.

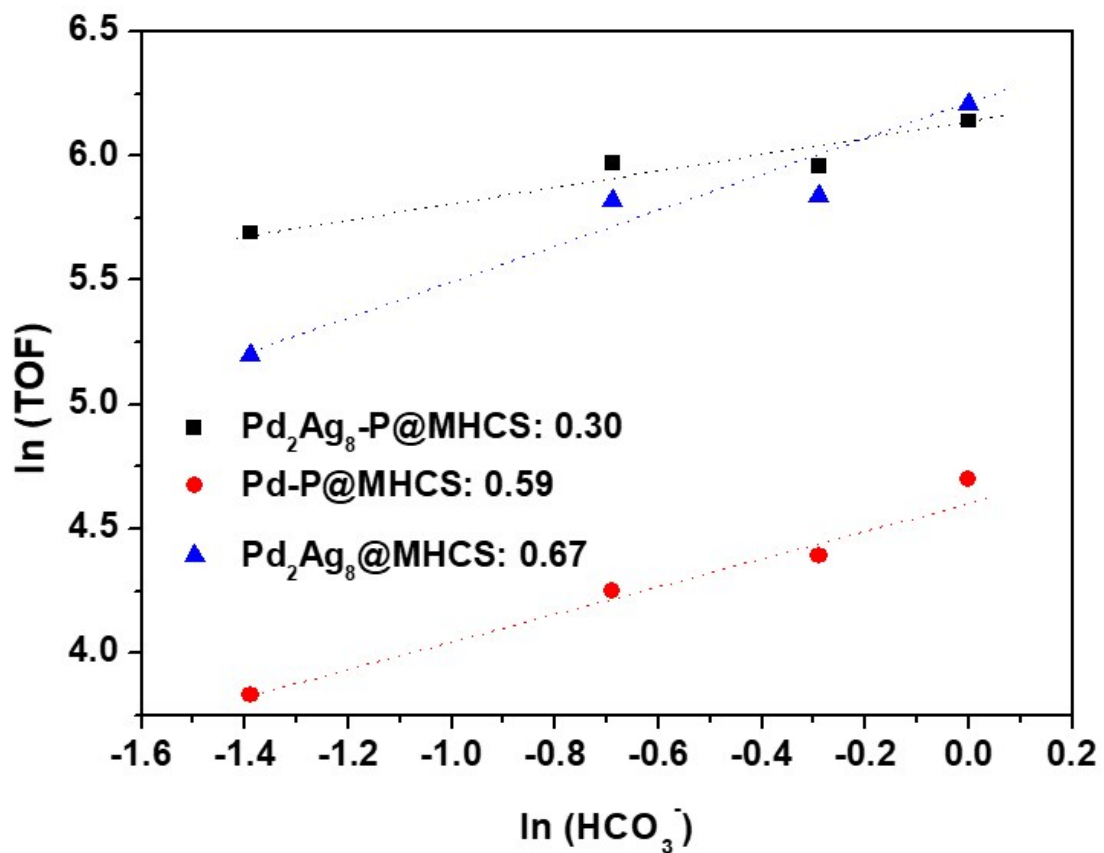


Figure S13. Effect of HCO_3^- concentration on TOF values using $\text{Pd}_2\text{Ag}_8\text{-P@MHCS}$, Pd-P@MHCS and $\text{Pd}_2\text{Ag}_8@\text{MHCS}$ catalysts. Reaction conditions: 10 mg catalyst, 0.25 M, 0.5 M, 0.75 M and 1.0 M aqueous NaHCO_3 solution (15 mL), H_2/CO_2 (1:1, total 2.0 MPa), 100 °C, 1 h.